JOURNAL OF Materials CHEMISTRY

Study on a series of pentanuclear planar 'open' clusters: synthesis, characterization, strong third-order optical nonlinearities and superior optical limiting properties

Chi Zhang,*[a,b,c] Yinglin Song,*[a] Fritz E. Kühn,*[b] Yuxiao Wang,[a] Hoongkun Fun[e] and Xinquan Xin[d]

[a]*Department of Applied Physics, Harbin Institute of Technology, Harbin 150001, P. R. China*
[b]*Anorganisch-Chemisches Institut der Technischen Universität München, Lichtenbergstrasse 4, D-85747 Garching bei München, Germany*
[c]*Department of Chemistry, University of Kansas, Lawrence, Kansas 66045, USA*
[d]*State Key Laboratory of Coordination Chemistry, Department of Chemistry, Nanjing University, Nanjing 210093, P. R. China*
[e]*X-Ray Crystallography Unit, School of Physics, Universiti Sains Malaysia 11800, USM, Penang, Malaysia*

Received 30th April 2001, Accepted 14th November 2001
First published as an Advance Article on the web 4th January 2002

A series of new candidates as nonlinear optical materials, heterothiometallic clusters $[MS_4Cu_4X_2(py)_6]$ (X = I, M = W, **1**, Mo, **2**; X = Br, M = W, **3**, Mo, **4**) have been synthesized *via* two comparative synthetic routes for third-order NLO studies. Single-crystal X-ray diffraction shows that the neutral clusters assume pentanuclear planar 'open' structures. Their optical responses to incident pulsed laser exhibit very large optical limiting effects, which are simulated by using excited-state absorption theory, with limiting thresholds of 0.07–0.10 J cm^{-2} for clusters **1–4**, and these effects should make this series of clusters among the most promising optical limiters. The strong third-order optical nonlinear absorption and optical self-focusing effects of clusters **1–4** in DMF solution were observed in the *Z*-scan measurements of an 8-ns pulsed laser at 532 nm. The corresponding effective third-order nonlinear optical susceptibilities of this series of clusters were found to be the largest among all kinds of heterothiometallic clusters, and their third-order nonlinear hyperpolarizabilities are also reported. The nonlinear effects for these four clusters in DMF solution have also been investigated by time-resolved pump–probe experiments to provide direct evidence on the physical origin of the observed OL effects. The nonlinear optical properties of this series of clusters **1–4** were compared with other NLO cluster compounds studied previously and revealed a qualitative structure/NLO property correlation.

Introduction

Inspired by the development of opto-electronic devices, tremendous interest has been aroused to search for new materials with third-order nonlinear optical (NLO) properties.[1] The potential applications in such materials are optical communication, optical signal processing and transmission, optical data acquisition and storage, optical computing, optic-electronic modulation,[2] and especially optical limiting (OL) effects utilized in the protection of optical sensors and human eyes from high-intensity laser beams.[3] In the past two decades, nonlinear optical research has been mainly focused on inorganic semiconductors, organic molecules, conjugated polymers and organometallic compounds.[4–6] With the progressive research in this active field, the design and synthesis of new molecular materials with large macroscopic optical nonlinearities mirror the subject of the current research interest, and represent a new active research field in modern chemistry, physics and materials science.

Only very recently, transition-metal sulfur clusters have been developed as a new promising class of nonlinear optical materials,[7] and gradually attracted much attention due to their possessing the combined advantages of both organic molecules and inorganic semiconductors: large modifiable structures and structures containing many heavy metal atoms. In these heterothiometallic clusters, one of the most important and promising features is the opportunity provided to modify and eventually optimize the building block through subtle modification achieved at the molecular level, therefore both the structural units and terminal ligands can be altered just as for organic molecules so that alteration of NLO properties can be realized through structural manipulation. On the other hand, incorporation of heavy metal atoms may introduce more sublevels into the energy hierarchy as compared to organic molecules with the same number of skeleton atoms, which permits more allowed electron transitions to take place and hence larger NLO effects especially those beneficial to NLO applications. Our studies on these clusters show that, unlike some traditional NLO materials, the skeletons and constituent elements in these clusters were found to have considerable influence on their NLO performance, which results in the Mo(W)/S/Cu(Ag) clusters exhibiting rather diverse combinations of NLO effects. Cubane-like,[7a,8] half-open cubane-like[9] and hexagonal prism-shaped clusters[10] show strong nonlinear absorption while strong nonlinear refraction effects are found in nest-shaped,[11] twin-nest-shaped[12] and butterfly-shaped clusters.[13] A twenty-nuclear supra-cage cluster[14] possesses a very large nonlinear susceptibility. Hexagonal prism-shaped clusters,[10] pentanuclear planar 'open' clusters[15] and cluster polymers[16] seem to reveal large optical limiting properties.

To further develop this promising field, and also to search for better NLO materials with larger OL properties, we have

DOI: 10.1039/b103839g

synthesized a series of pentanuclear clusters **1–4** with planar 'open' skeletons by ligand-redistribution and solid-state reactions, and characterized their structures by X-ray crystallographic determination. The results of *Z*-scan experiments show that these clusters possess strong NLO absorptive abilities and effective optical self-focusing behaviors, and comparison of optical nonlinearities has therefore been made among the various skeletons of heterothiometallic clusters. The superior optical limiting effects of this series of clusters are observed in the OL measurements, which are simulated by using excited-state absorption theory, and are comparable to those of well-known OL materials. Their largest third-order nonlinear optical susceptibilities $\chi^{(3)}$ among all the heterothiometallic clusters also qualify the present clusters as very promising optical limiters. Time-resolved pump–probe experiments have been conducted on this series of clusters to give direct evidence on the physical origin of the observed OL effects.

Experimental

General

All reactions and manipulations were conducted using standard Schlenk techniques under an atmosphere of nitrogen. The compounds $(R_4N)_2MS_4$ (M = W, Mo; R = H, Et) were prepared according to literature.[17] The solvents were carefully dried and distilled prior to use, and other chemicals were generally used as commercially available.

Preparation of $[WS_4Cu_4I_2(py)_6]$ 1 (method 1)

CuI (2 mmol, 0.38 g) was added to pyridine (15 cm^3), and the solution was stirred for *ca.* 5 min at room temperature. The system changed from colorless to light yellow and the CuI dissolved completely. Then $(NH_4)_2WS_4$ (0.5 mmol, 0.174 g) was added. The reacting system immediately turned to deep-red and was stirred for additional 10 min. The resulting solution was subsequently filtered to afford a deep-red filtrate. Deep-red crystals were obtained after several days by layering the filtrate with i-PrOH. Yield: 0.60 g (92%). Anal. Calc. for $C_{30}H_{30}N_6I_2Cu_4S_4W$: C, 27.83; H, 2.34; N, 6.49%. Found: C, 27.66; H, 2.51; N, 6.31%. UV-vis (DMF, λ_{max}/nm, 10^3 ε/dm^3 mol^{-1} cm^{-1}): 438 (8.5), 316 (32.0). IR (KBr pellets, cm^{-1}): 1597(vs), 1482(s), 1441(vs), 1211(s), 1067(s), 1037(s), 1009(s), 751(vs), 696(vs), 626(s), 437(vs) [ν(W–μ_3-S)].

Preparation of $[MoS_4Cu_4I_2(py)_6]$ 2 (method 1)

The same procedure as for the preparation of cluster **1** was employed to synthesize cluster **2** except that $(NH_4)_2MoS_4$ (0.5 mmol, 0.130 g) was used instead of $(NH_4)_2WS_4$. Black-red crystals were isolated. Yield: 0.57 g (94%). Anal. Calc. for $C_{30}H_{30}N_6I_2Cu_4S_4Mo$: C, 29.83; H, 2.49; N, 6.76%. Found: C, 29.71; H, 2.33; N, 6.75%. UV-vis (DMF, λ_{max}/nm, 10^3 ε/dm^3 mol^{-1} cm^{-1}): 526 (3.7), 384 (11.1), 298 (26.1). IR (KBr pellets, cm^{-1}): 1597(vs), 1482(s), 1441(vs), 1215(s), 1066(s), 1036(s), 1009(s), 751(vs), 696(vs), 626(s), 447(vs) [ν(Mo–μ_3-S)].

Preparation of $[WS_4Cu_4Br_2(py)_6]$ 3 (method 1)

The same procedure as for the preparation of cluster **1** was employed to synthesize cluster **3** except that CuBr (2 mmol, 0.287 g) was used instead of CuI. Deep-red crystals were isolated. Yield: 0.57 g (95%). Anal. Calc. for $C_{30}H_{30}N_6Br_2Cu_4S_4W$: C, 29.83; H, 2.49; N, 6.96%. Found: C, 29.71; H, 2.33; N, 6.85%. UV-vis (DMF, λ_{max}/nm, 10^3 ε/dm^3 mol^{-1} cm^{-1}): 442 (2.2), 334 (5.1). IR (KBr pellets, cm^{-1}): 1597(vs), 1482(s), 1441(vs), 1214(s), 1066(s), 1036(s), 1009(s), 751(vs), 696(vs), 626(s), 437(vs) [ν(W–μ_3-S)].

Preparation of $[MoS_4Cu_4Br_2(py)_6]$ 4 (method 1)

The same procedure as for the preparation of cluster **3** was employed to synthesize cluster **4** except that $(NH_4)_2MoS_4$ (0.5 mmol, 0.130 g) was used instead of $(NH_4)_2WS_4$. Black-red crystals were isolated. Yield: 0.51 g (92%). Anal. Calc. for $C_{30}H_{30}N_6Br_2Cu_4S_4Mo$: C, 32.37; H, 2.70; N, 7.55%. Found: C, 32.45; H, 2.61; N, 7.31%. UV-vis (DMF, λ_{max}/nm, 10^3 ε/dm^3 mol^{-1} cm^{-1}): 524 (1.3), 372 (3.3), 292 (10.1). IR (KBr pellets, cm^{-1}): 1597(vs), 1482(s), 1441(vs), 1214(s), 1066(s), 1036(s), 1009(s), 751(vs), 696(vs), 625(s), 447(vs) [ν(Mo–μ_3-S)].

Preparation of 1–4 (method 2)

A well-ground mixture of $(Et_4N)_2MS_4$ (M = W, Mo) (0.5 mmol, 0.287 g, W; 0.243 g, Mo), CuI (2 mmol, 0.38 g) or CuBr (2 mmol, 0.287 g) was put into a reaction tube and heated to 90 °C for 8 h under a nitrogen atmosphere. After extracting the resultant black solid with pyridine (20 cm^3), the extract was filtered to afford a deep (or black) red filtrate. Single crystals were obtained after several days by layering the filtrate with i-PrOH. Yield: 0.50 g (78%) **1**; 0.45 g (75%) **2**; 0.47 g (78%) **3**; 0.42 g (75%) **4**.

Crystal structure determinations

A well-developed single crystal of a given cluster with suitable dimensions was mounted on a glass fiber and diffraction data were collected at 20 ± 2 °C on a Siemens Smart CCD area-detector diffractometer in the range $2.84 < 2\theta < 56.54°$ (**1**), $2.88 < 2\theta < 56.72°$ (**3**, **4**) by using an ω-scan technique. The data reductions were performed on a Silicon Graphics Indy workstation with Smart-CCD software. The structures were solved by the direct method and refined by full-matrix-least-squares on F^2 using the SHELXTL-PC (Version 5.1) package of crystallographic software.[18] All non-hydrogen atoms were refined anisotropically. The hydrogen atoms were generated and included in the structure factor calculations with assigned isotropic thermal parameters but were not refined. The data processing and structure refinement parameters are listed in Table 1.

CCDC reference numbers 156623–156625. See http://www.rsc.org/suppdata/jm/b1/b103839g/ for crystallographic data in CIF or other electronic format.

Other characterisation measurements

Elemental analysis for carbon, hydrogen and nitrogen were performed on a Perkin-Elmer 240C elemental analyzer. Infrared spectra were recorded with a Nicolet FT-170SX Fourier transform spectrometer (KBr pellets). Electronic spectra were measured on a Shimazu UV-3100 spectrophotometer.

Optical measurements

A DMF solution of clusters **1–4** was placed in a 5-mm quartz cuvette for optical limiting property measurements which were performed with linearly polarized 8-ns pulses at 532 nm generated from a Q-switched frequency-doubled Nd : YAG laser. The clusters **1–4** are stable toward air and laser light under the experimental conditions. The spatial profiles of the optical pulses were of nearly Gaussian transverse mode. The pulsed laser was focused onto the sample cell with a 30 cm focal length mirror. The spot radius of the laser beam was measured to be 55 μm (half-width at $1/e^2$ maximum). The energy of the input and output pulses were measured simultaneously by precision laser detectors (Rjp-735 energy probes) which were linked to a computer by an IEEE interface,[19] while the incident pulse energy was varied by a Newport Com. Attenuator. The interval between the laser pulses was chosen to be 1 s to avoid the influence of thermal and long-term effects.

Table 1 Crystallographic data for $[WS_4Cu_4I_2(py)_6]$ **1**, $[WS_4Cu_4Br_2(py)_6]$ **3** and $[MoS_4Cu_4Br_2(py)_6]$ **4**

Compound	**1**	**3**	**4**
Data collection	Siemens Smart CCD diffractometer ω-scans	Siemens Smart CCD diffractometer ω-scans	Siemens Smart CCD diffractometer ω-scans
Radiation	Mo-Kα (λ = 0.71073 Å)	Mo-Kα (λ = 0.71073 Å)	Mo-Kα (λ = 0.71073 Å)
Chemical formula	$C_{30}H_{30}Cu_4I_2N_6S_4W$	$C_{30}H_{30}Cu_4Br_2N_6S_4W$	$C_{30}H_{30}Cu_4Br_2N_6S_4Mo$
Formula weight	1294.65	1200.67	1112.76
Crystal color and habit	Deep red block	Deep red block	Dark red block
Crystal dimensions / mm	0.42 × 0.40 × 0.36	0.52 × 0.34 × 0.24	0.30 × 0.28 × 0.28
Crystal system	Orthorhombic	Orthorhombic	Orthorhombic
Space group	*Fdd*2	*Fdd*2	*Fdd*2
a/Å	22.61310(10)	22.58970(10)	22.54960(10)
b/Å	23.0681(3)	22.8053(3)	22.7445(3)
c/Å	30.8375(4)	30.1995(3)	30.2498(4)
V/Å^3	16086.1(3)	15557.7(3)	15514.5(3)
T/K	293	293	293
Z	16	16	16
D_c/g cm^{-3}	2.138	2.050	1.906
F(000)	9792	9216	8704
μ/cm^{-1}	6.703	7.397	4.778
Index ranges	$-29 \leqslant h \leqslant 30$, $-30 \leqslant k \leqslant 30$, $-41 \leqslant l \leqslant 25$	$-18 \leqslant h \leqslant 30$, $-30 \leqslant k \leqslant 30$, $-40 \leqslant l \leqslant 40$	$-30 \leqslant h \leqslant 19$, $-30 \leqslant k \leqslant 27$, $-38 \leqslant l \leqslant 40$
Reflections collected/unique	27527, 8372 (R_{int} = 0.0446)	26507, 9516 (R_{int} = 0.0593)	26474, 9414 (R_{int} = 0.0457)
Absorption correction	Empirical	Empirical	Empirical
Data/restraints/parameters	8372, 1, 425	9516, 1, 426	9414, 1, 425
Goodness-of-fit on F^2	1.097	1.008	1.042
Final *R* indices [$I > 2\sigma(I)$]	R_1 = 0.0352, wR_2 = 0.0761	R_1 = 0.0432, wR_2 = 0.0977	R_1 = 0.0479, wR_2 = 0.0966
Largest diff. peak and hole/e Å^{-3}	0.632, −1.122	0.911, −0.662	0.815, −0.418

The third-order NLO absorptive and refractive properties of clusters **1–4** were determined by performing *Z*-scan measurements.[20] The samples were mounted on a translation stage that was controlled by the computer to move along the axis of the incident laser beam (*Z*-direction) with respect to the focal point instead of being positioned at its focal point. For determining both the sign and magnitude of the nonlinear refraction, a 0.2 mm diameter aperture was placed in front of the transmission detector and the transmittance recorded as a function of the sample position on the *Z* axis (closed-aperture *Z*-scan). For measuring the nonlinear absorption, the *Z*-dependent sample transmittance was taken without the aperture (open-aperture *Z*-scan).

Results and discussion

Synthetic reactions

Our previous research on the optical limiting (OL) properties and NLO effects of heterothiometallic clusters demonstrated that incorporation of heavy atoms into these clusters may be responsible for improvement of their NLO behaviors especially in their OL properties. With these in mind, we synthesized the clusters $[MS_4Cu_4X_2(py)_6]$ by using two comparative routes, ligand-redistribution reaction and solid-state reaction, to replace lighter halogen or pseudo halogen group NCS^- with heavier X^-. In method 1, the starting material CuX reacted with py, which exhibits a strong super-conjugation effect in the py ring that may result in py possessing a high tendency to coordinate with the Cu atom. The gradual dissolving of CuX and the formation of a light yellow solution was consistent with the formation of the intermediate product $CuX(py)_3$.[21] Then the synthon thiometallate $[MS_4]^{2-}$ as a bidentate ligand[22] was added to the reaction system. The solution immediately turned from light-yellow to deep (or black) red in color, which suggested that the target cluster compounds were formed. Since the sequence of some Cu(I)-philic ligands of Mo(W)/S/Cu(Ag) compounds can be regarded as the following: S^{2-} > (py, PPh_3) > X^- (X = Cl, Br, I, CN), the former ligands can substitute part or all of the latter ligands, while the required coordination number of copper is not more than four. Two bonds of the $CuX(py)_3$ were broken by the attack of S^{2-} from the $[MS_4]^{2-}$ moiety. On the basis of our hypothesis, there is

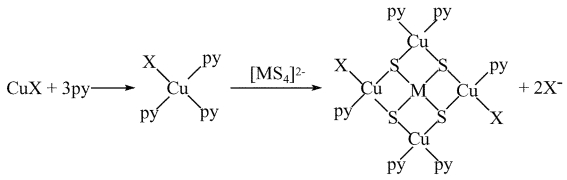

Scheme 1

almost the same probability in the formation of units [CuX(py)] and $[Cu(py)_2]$, which have the same chance (1 : 1) to further coordinate with the $[MS_4]^{2-}$ moiety to form the final products with a symmetrical skeleton $[MS_4Cu_4X_2(py)_6]$ Scheme 1). In contrast to method 1, the low-heat solid-state synthesis method 2, developed by our laboratory, was also used to prepare clusters **1–4** by reacting starting material CuX with the synthon $[MS_4]^{2-}$ to first form the cluster skeleton $[MS_4(CuX)_4]^{2-}$. Then the intermediate was treated with py by partially substituting the X^- with py, due to py showing stronger coordination with Cu than X^-, to give the final planar 'open' shaped clusters. (Scheme 2).

It is noted that the target heterothiometallic clusters were prepared in very high yield (>90%) (method 1), which is seldom observed in preparing Mo(W)/S/Cu(Ag) hetero-bimetallic clusters *via* various synthetic routes. The adoption of synthetic method 1 seems to be profitable for ensuring almost all the CuX coordinates with the excess py and then further reacts with the synthon $[MS_4]^{2-}$ unit. All procedures are conducted under an inert atmosphere in order to avoid the formation of the blue Cu(II) complexes.

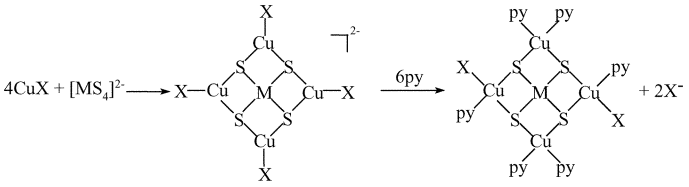

Scheme 2

Crystal structures

The crystal structures of the neutral clusters $[MS_4Cu_4X_2(py)_6]$ (M = W, Mo; X = I, Br) determined by X-ray diffraction are isomorphous and only the structures of **1** and **4** are shown in Figs. 1 and 2, with their selected bond lengths and bond angles listed in Table 2. These four heterothiometallic clusters can be described as pentanuclear planar 'open' structures. The skeleton is composed of one M (M = Mo, W), four Cu and four S atoms to form a MS_4Cu_4 aggregate, in which the M atom is in the center of the clusters while both the M and Cu atoms are essentially tetrahedrally coordinated. The neutral structures of these clusters are of pseudo D_{2d} symmetry and the five metal atoms are nearly co-planar with deviations of not more than 0.1 Å from the least-squares plane. This is correlative with the fact that the angles of Cu(1)–M1–Cu(1A) and Cu(2)–M1–Cu(2A) are 178.76(6) and 174.92(6)° in Mo-containing cluster **4**, 178.06(5), 173.50(5)° and 178.42(7), 174.53(6)° in W-containing clusters **1** and **3**, respectively. Each of the two mutual *trans* Cu(2) and Cu(2A) atoms is linked with two μ_3-S atoms, one X atom and one pyridine ligand to form a distorted tetrahedral $S_2CuX(py)$ unit. Each of the other two Cu(1) and Cu(1A) atoms is coordinated by two μ_3-S atoms and two pyridine ligands building up a distorted tetrahedral $S_2Cu(py)_2$ moiety. A couple of $S_2CuX(py)$ units and $S_2Cu(py)_2$ units ligate through four of the six edges of the tetrahedral $[MS_4]^{2-}$ moiety. The M–S bond lengths and the S–M–S angles

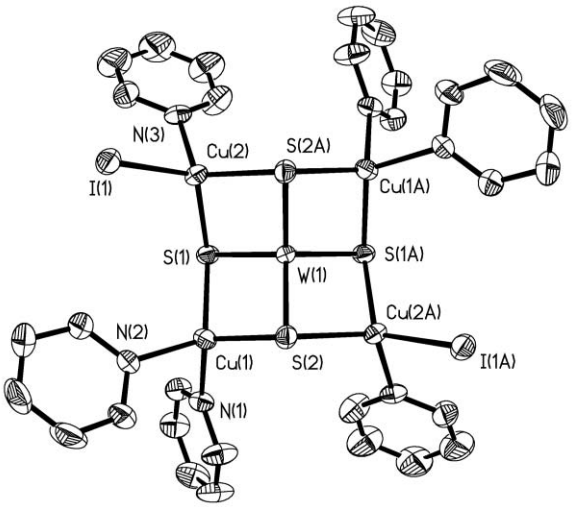

Fig. 1 A perspective view of the structure of the neutral cluster $[WS_4Cu_4I_2(py)_6]$ **1**.

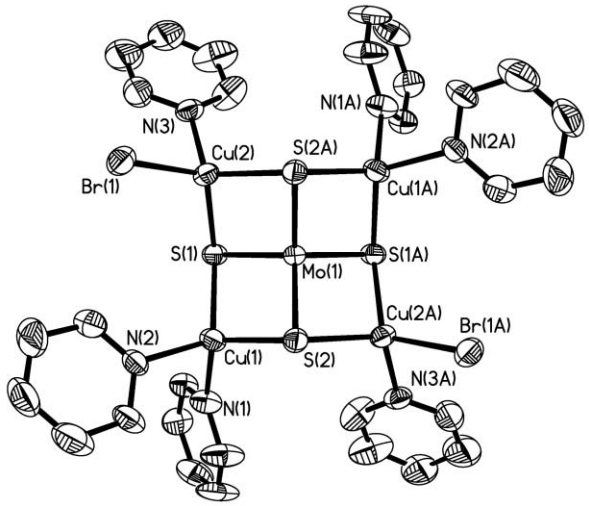

Fig. 2 A perspective view of the structure of the neutral cluster $[MoS_4Cu_4Br_2(py)_6]$ **4**.

Table 2 Selected bond lengths (Å) and bond angles (°) for $[WS_4Cu_4I_2(py)_6]$ **1**, $[WS_4Cu_4Br_2(py)_6]$ **3** and $[MoS_4Cu_4Br_2(py)_6]$ **4** (X = I, M = W, **1**; X = Br, M = W, **3**, Mo, **4**)

	1	**3**	**4**
M(1)–Cu(1)	2.6990(8)	2.6879(12)	2.6732(10)
M(1)–Cu(2)	2.7431(9)	2.7300(11)	2.7116(9)
M(1)–S(1)	2.240(2)	2.242(3)	2.238(2)
M(1)–S(2)	2.236(2)	2.232(3)	2.233(2)
Cu(1)–S(1)	2.294(2)	2.295(3)	2.275(2)
Cu(1)–S(2)	2.282(2)	2.282(3)	2.267(2)
Cu(1)–N(1)	2.096(6)	2.109(9)	2.107(7)
Cu(1)–N(2)	2.051(7)	2.051(9)	2.054(7)
Cu(2)–N(3)	2.073(6)	2.066(9)	2.076(7)
Cu(2)–X(1)	2.6448(11)	2.4653(17)	2.4634(13)
Cu(2)–S(1)	2.327(2)	2.311(3)	2.296(2)
Cu(2)–S(2A)	2.318(2)	2.304(3)	2.294(2)
S(2)–M(1)–S(1)	108.67(7)	108.39(9)	108.43(8)
S(1)–M(1)–S(1A)	111.36(12)	111.23(16)	111.98(12)
S(2)–M(1)–S(2A)	111.21(12)	111.05(16)	111.31(12)
Cu(1)–M(1)–Cu(1A)	178.06(5)	178.42(7)	178.76(6)
Cu(1)–M(1)–Cu(2)	91.86(3)	91.61(4)	91.54(3)
Cu(1)–M(1)–Cu(2A)	88.25(3)	88.47(4)	88.52(3)
Cu(2)–M(1)–Cu(2A)	173.50(5)	174.53(6)	174.92(6)
N(1–Cu(1)–N(2)	97.9(2)	97.2(3)	97.6(3)
N(1)–Cu(1)–S(2)	118.2(2)	119.8(3)	119.2(2)
N(1)–Cu(1)–S(1)	106.72(19)	105.3(3)	105.4(2)
N(2)–Cu(1)–S(2)	110.7(2)	111.1(3)	111.0(2)
N(2)–Cu(1)–S(1)	118.8(2)	118.7(3)	118.0(2)
N(3)–Cu(2)–S(1)	101.3(2)	102.7(3)	103.0(2)
N(3)–Cu(2)–S(2A)	121.1(2)	120.2(3)	119.8(2)
S(2)–Cu(1)–S(1)	105.06(7)	105.33(10)	106.00(8)
S(2A)–Cu(2)–S(1)	103.04(7)	103.64(10)	104.35(8)
S(2A)–Cu(2)–X(1)	104.44(6)	105.92(10)	105.70(7)
Cu(1)–S(1)–Cu(2)	110.14(10)	110.27(13)	110.64(10)
N(3)–Cu(2)–X(1)	104.4(2)	102.5(3)	102.7(2)
S(1)–Cu(2)–X(1)	124.15(6)	123.31(9)	122.51(7)

are quite similar, which also suggests that the MS_4 cores still retain their tetrahedral coordinated geometry.

Nonlinear optical properties

Electronic spectra

The similarity in the structures of these clusters also leads to similar electronic spectra as confirmed in Fig. 3. The red shifts in the spectra of clusters **2** and **4** are expected since they contain a Mo atom instead of a W atom.[22] The lowest energy absorption peaks of these four clusters located at 526 nm **2**, 524 nm **4** and 438 nm **1**, 442 nm **3** respectively, can be assigned as charge-transfer bands of the type $(\pi)S \rightarrow (d)M$ (M = Mo, W) arising from the MS_4 moiety and all of them are red-shifted compared to those of the free $[MS_4]^{2-}$ anion (472 nm for Mo and 397 nm for W).[17] The electronic spectra of these four clusters show relatively low linear absorption in the visible and near-IR regions, suggesting low intensity loss and little temperature change caused by photon absorption when pulsed light propagates in the materials, which indicates the clusters are good potential optical limiters.

Nonlinear optical absorption and refraction

The nonlinear optical (NLO) properties of the clusters **1–4** were investigated with 532 nm laser pulses of 8-ns duration in 5.50×10^{-4}, **1** (1.39×10^{-4}, **2**; 2.83×10^{-4}, **3**; and 3.8×10^{-4}, **4**) mol dm^{-3} DMF solution. The typical results of the *Z*-scan experiments[20] of clusters **1–4** are displayed in Figs. 4–7. The optical propagation equation for the pulsed light intensity is given by eqn. (1):[23]

$$\frac{dI}{dz} = -\alpha I \quad (1)$$

where α is the non-linear absorption coefficient of the samples,

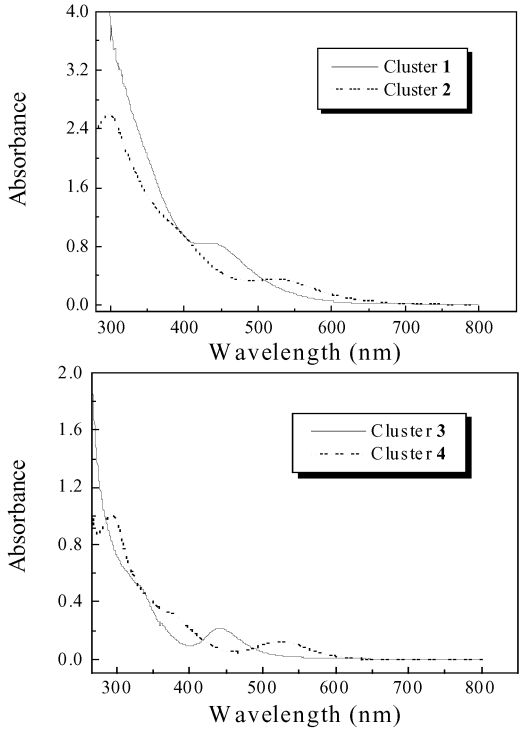

Fig. 3 Electronic spectra of $[MS_4Cu_4X_2(py)_6]$ (X = I, M = W, **1**, Mo, **2**; X = Br, M = W, **3**, Mo, **4**) in DMF solution with 1 cm optical pathlength. The concentrations of clusters **1–4** are 1.0×10^{-4} mol dm^{-3}.

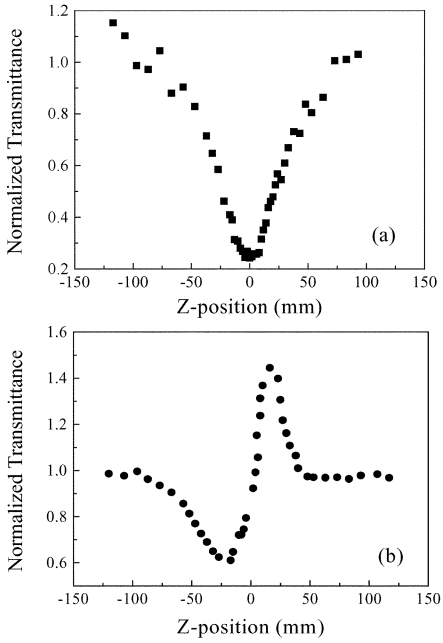

Fig. 4 *Z*-Scan data of a 5.50×10^{-4} mol dm^{-3} DMF solution of $[WS_4Cu_4I_2(py)_6]$ at 532 nm with $I_0 = 8.2 \times 10^{12}$ mol dm^{-3}: (a) collected under the open aperture configuration showing NLO; (b) obtained by dividing the normalized *Z*-scan data obtained under closed aperture configuration by the normalized *Z*-scan data in (a) (this shows the self-focusing effect of cluster **1**).

which can be expressed as the function of the incident pulsed light intensity I from eqn. (2):[23]

$$\alpha = \alpha_0 + \frac{1 + K_\alpha \frac{I}{I_s}}{1 + \frac{I}{I_s}} \sigma_0 N \tag{2}$$

In the eqn. (2), α_0 is the linear absorption coefficient of the sample, σ_0 is the absorption cross-section of the ground-state molecular solution, N is the concentration of the cluster sample solution, $I_s = h\gamma/\sigma_0\tau_{e0}$ is the saturation intensity, with τ_{e0} being the lifetime of the excited-state, $K_\alpha = \sigma_e/\sigma_0$ is the ratio of the excited-state absorption cross-section to the ground-state cross-section.

The nonlinear absorption components were evaluated by the *Z*-scan method under an open aperture configuration (Figs. 4a, 5a, 6a, 7a) and the NLO absorptive experimental data for clusters **1–4** obtained under the conditions used in this study can be well described by eqns. (3) and (4),[20,24] which are used to describe a third-order NLO absorptive process:

$$T(Z) = \frac{1}{\sqrt{\pi} q(Z)} \int_{-\infty}^{+\infty} \ln[1 + q(Z) e^{-\tau^2}] d\tau \tag{3}$$

$$q(Z) = \int_0^{+\infty} \int_0^{+\infty} \alpha_2 \frac{I_0}{1 + (Z/Z_0)^2} e^{[-2(\gamma/\varpi_0)^2 - (t/t_0)^2]} \frac{1 - e^{-\alpha_0 L}}{\alpha_0} r dr dt \tag{4}$$

where light transmittance T is a function of the sample's *Z*-position (against focal point $Z = 0$), Z is the distance of the sample from the focal point, L is the sample thickness, I_0 is the peak irradiation intensity at focus. $Z_0 = \pi\omega_0^2/\lambda$, where ω_0 is the spot radius of the laser pulse at focus and λ is the laser wavelength. r is the radial coordinate, t is the time, t_0 is the pulse width.

The nonlinear refractive properties of clusters **1–4** were assessed by dividing the normalized *Z*-scan data obtained under the closed aperture configuration by the normalized *Z*-scan data obtained under the open aperture configuration (Figs. 4b, 5b, 6b, 7b). The valley/peak patterns of the corrected transmittance curves show characteristic self-focusing behaviors of the propagating light in the samples. An effective third-order nonlinear refractive index n_2 of clusters **1–4**, can be derived from the difference between normalized transmittance values at valley and peak position (ΔT_{v-p}) by use of eqn. (5):[25]

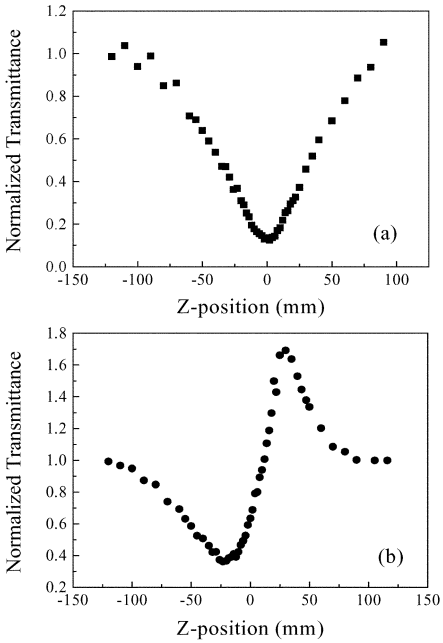

Fig. 5 *Z*-Scan data of a 1.39×10^{-4} mol dm^{-3} DMF solution of $[MoS_4Cu_4I_2(py)_6]$ at 532 nm with $I_0 = 8.2 \times 10^{12}$ mol dm^{-3}: (a) collected under the open aperture configuration showing NLO; (b) obtained by dividing the normalized *Z*-scan data obtained under closed aperture configuration by the normalized *Z*-scan data in (a) (this shows the self-focusing effect of cluster **2**).

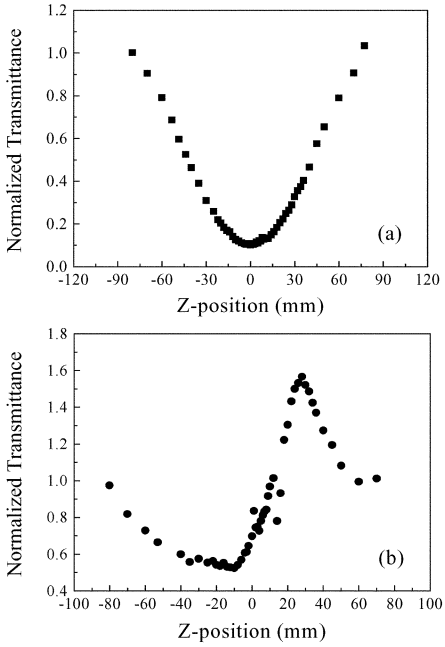

Fig. 6 *Z*-Scan data of a 2.83×10^{-4} mol dm^{-3} DMF solution of $[WS_4Cu_4Br_2(py)_6]$ at 532 nm with $I_0 = 8.2 \times 10^{12}$ mol dm^{-3}: (a) collected under the open aperture configuration showing NLO; (b) obtained by dividing the normalized *Z*-scan data obtained under closed aperture configuration by the normalized *Z*-scan data in (a) (this shows the self-focusing effect of cluster **3**).

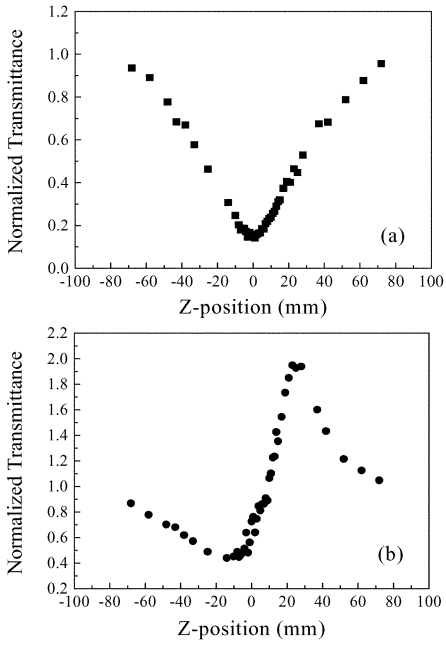

Fig. 7 *Z*-Scan data of a 3.8×10^{-4} mol dm^{-3} DMF solution of $[MoS_4Cu_4Br_2(py)_6]$ at 532 nm with $I_0 = 8.2 \times 10^{12}$ mol dm^{-3}: (a) collected under the open aperture configuration showing NLO; (b) obtained by dividing the normalized *Z*-scan data obtained under closed aperture configuration by the normalized *Z*-scan data in (a) (this shows the self-focusing effect of cluster **4**).

$$n_2 = \frac{\lambda\alpha_0}{0.812\pi I(1-e^{-\alpha_0 L})}\Delta T_{V-P} \quad (5)$$

Figs. 4–7 show the typical NLO absorptive and refractive effects of clusters **1–4**, respectively, in which, the filled squares and circles are the experimental data from the *Z*-scan measurements. Figs. 4a, 5a, 6a and 7a display the experimental data collected under an open aperture configuration (filled squares). Figs. 4b, 5b, 6b and 7b depict the data obtained by dividing the normalized *Z*-scan data under the closed aperture configuration by the normalized *Z*-scan data of (a) (filled circles). The NLO absorptive coefficients α_2 of clusters **1–4** were calculated to be 2.55×10^{-9}, 1.0×10^{-9}, 1.6×10^{-9}, 1.5×10^{-9} m W^{-1}, respectively. With the measured values of the difference of normalized transmittance values at valley and peak positions ΔT_{v-p} = 1.2 **1**, 1.1 **2**, 1.1 **3**, 1.2 **4**, the NLO refractive indices n_2 were calculated to be 8.2×10^{-9} esu **1**, 1.8×10^{-8} esu **2**, 7.8×10^{-9} esu **3**, 1.3×10^{-8} esu **4**, respectively. Obviously, clusters **1–4** possess very strong nonlinear absorption and self-focusing effects.

Comparing the NLO data of clusters **1–4**, the nonlinear absorption properties of clusters **1** and **3** are stronger than those of clusters **2** and **4**, whereas the nonlinear refractive capabilities of clusters **2** and **4** are larger than those of clusters **1** and **3**. The positive values of the third-order nonlinear refraction of clusters **1–4** also indicate that there are self-focusing effects in the NLO refractive behavior of this series of clusters. In accordance with the observed α_2 and n_2 values, the modulus of the effective third-order susceptibility $\chi^{(3)}$ can be calculated by eqn. (6).[9c,20]

$$|\chi^{(3)}| = \sqrt{\left(\left|\frac{9\times10^8\varepsilon_0 n_0^2 c^2}{2v}\alpha_2\right|^2 + \left|\frac{cn_0^2}{80\pi}n_2\right|^2\right)} \quad (6)$$

where v is frequency of the laser light, n_0 is the linear refractive index of the sample, ε_0 and c are the permittivity and the speed of the light in a vacuum, respectively. For 5.50×10^{-4} **1**, 1.39×10^{-4} **2**, 2.83×10^{-4} **3**, 3.8×10^{-4} mol dm^{-3} **4** as DMF solutions, the $\chi^{(3)}$ parameters were calculated to be 6.2×10^{-9} esu **1**, 5.9×10^{-9} esu **2**, 5.0×10^{-9} esu **3**, 4.62×10^{-9} esu **4**. The corresponding modulus of the hyperpolarizabilities γ of 6.9×10^{-30} esu **1**, 5.8×10^{-30} esu **2**, 1.27×10^{-30} esu **3**, 1.17×10^{-30} esu **4**, were obtained from $\chi^{(3)} = \gamma \cdot NF^4$, where N is the number density (concentration) of the clusters in the samples, $F^4 = 3.3$ is the local field correction factor. For making the comparison of the NLO effects, the NLO values α_2, n_2, $\chi^{(3)}$ and γ of this series of clusters as well as other different structural clusters such as nest-shaped, linear, cubane-like, half-open cubane-like, twin-nest, hexagonal-prism, butterfly and twenty-nuclear cage-shaped, are listed in Table 3. It is well known that the nonlinear optical processes of NLO materials are governed by the nonlinear susceptibility ($\chi^{(3)}$).[27] The larger the $\chi^{(3)}$ value, the better the material NLO properties. The $\chi^{(3)}$ value of some of the best performing, neat NLO materials such as semiconductors GaAs, Ge and organic polymers PA, PTS, PDA-4BCMU are 4.8×10^{-10}, 4.0×10^{-10}, 5.0×10^{-10}, 8.0×10^{-10} and 1.8×10^{-10} esu, respectively.[4d,28] Our recent work has shown that inorganic clusters also exhibit very large $\chi^{(3)}$ values, for example, 5.4×10^{-10} esu for the half-open cubane-like cluster $[Et_4N]_3[MoOS_3(CuBr)_3(\mu_2\text{-}Br)]$,[9a] 1.2×10^{-10} esu for the butterfly shaped cluster $[MoOS_3Cu_2(PPh_3)_3]$,[13a] 7.9×10^{-11} esu for the nest shaped cluster $[WOS_3Cu_3I(py)_5]$,[11b] 1.6×10^{-10} esu for the twin-nest shaped cluster $[Et_4N]_4[Mo_2O_2S_6Cu_6I_6]$,[12a] 5.6×10^{-10} esu for the hexagonal-prism shaped cluster $[Mo_2Ag_4S_8(PPh_3)_4]$,[10b] and the largest value reported for an inorganic cluster 8.2×10^{-10} esu for a twenty-nuclear supra-cage-shaped cluster $[Bu_4N]_4[Mo_8Cu_{12}O_8S_{24}]$.[14] Obviously, the $\chi^{(3)}$ values of clusters **1–4** are the largest of all the inorganic clusters. It should be noted that the values of these heterothiometallic clusters were determined only in $\sim 10^{-4}$ mol dm^{-3} dilute solution. A much larger $\chi^{(3)}$ value can be expected if a higher concentration can be achieved. Table 3 also indicates that the more complicated the structural skeleton and the more heavy atoms the heterobimetallic

Table 3 Nonlinear optical parameters of the heterothiometallic cluster compounds measured at 532 nm with nanosecond-duration laser pulses

Compound	Structure type	α_2/m W^{-1}	n_2/esu	$\chi^{(3)}$/esu	γ/esu	N/mol dm^{-3}	Ref.
$[MoOS_3Cu_2(PPh_3)_3]$	Butterfly	2.6×10^{-11}	3.6×10^{-9}	1.2×10^{-10}	9.8×10^{-28}	[a] 7.4×10^{-5}	13*a*
$[WOS_3Cu_2(PPh_3)_4]$	Butterfly	$< 10^{-12}$	5.9×10^{-10}	2×10^{-11}	9.0×10^{-29}	[a] 1.2×10^{-4}	13*a*
$[Et_4N]_3[MoOS_3(CuBr)_3(\mu_2\text{-Br})]$	Half-open cubane	1.6×10^{-10}	-1.6×10^{-8}	5.4×10^{-10}	1.6×10^{-28}	[a] 1.9×10^{-3}	9*a*
$[Et_4N]_3[WOS_3(CuBr)_3(\mu_2\text{-Br})]$	Half-open cubane	6.0×10^{-10}	7.9×10^{-9}	2.6×10^{-10}	1.6×10^{-28}	[a] 9.1×10^{-4}	9*b*
$[Et_4N]_3[WOS_3(CuI)_3(\mu_2\text{-I})]$	Half-open cubane	1.0×10^{-10}	-3.6×10^{-10}	1.2×10^{-11}	2.8×10^{-29}	[a] 2.3×10^{-4}	9*c*
$[MoOS_3Cu_3I(py)_5]$	Nest shaped	6.5×10^{-10}	-2.2×10^{-9}	7.5×10^{-11}	5.8×10^{-27}	[a] 2×10^{-4}	11*b*
$[WOS_3Cu_3I(py)_5]$	Nest shaped	3.5×10^{-10}	2.6×10^{-9}	7.9×10^{-11}	2.2×10^{-27}	[b] 1.7×10^{-4}	11*b*
$[MoOS_3Cu_3(4\text{-pic})_6]\cdot Br$	Nest-shaped	1.6×10^{-10}	3.2×10^{-8}	5.4×10^{-12}	2.51×10^{-31}	[d] 3.86×10^{-4}	26
$[WOS_3Cu_3(4\text{-pic})_6]\cdot Br$	Nest-shaped	2.8×10^{-10}	3.3×10^{-8}	5.5×10^{-12}	1.03×10^{-31}	[d] 8.89×10^{-4}	26
$[Et_4N]_4[Mo_2O_2S_6Cu_6I_6]$	Twin-nest shaped	4×10^{-10}	-4.3×10^{-9}	1.6×10^{-10}	—	[a] 2×10^{-3}	12*a*
$[MoOS_3Cu_3(PPh_3)_3\{S_2P(OBu)_2\}]$	Cubane-like	5×10^{-10}	$< 7.1 \times 10^{-12}$	2×10^{-11}	—	[b] 1.0×10^{-4}	8*c*
$[MoS_4Cu_2Ag(PPh_3)_3]\cdot Br$	Cubane-like	8×10^{-10}	2.7×10^{-8}	4.5×10^{-10}	—	[a] 4.5×10^{-4}	8*c*
$[Mo_2Ag_4S_8(PPh_3)_4]$	Hexagonal-prism	1.8×10^{-9}	1.6×10^{-8}	5.6×10^{-10}	—	[c] 1.3×10^{-4}	10*b*
$[W_2S_8Ag_4(AsPh_3)_4]$	Hexagonal-prism	2.8×10^{-9}	4.2×10^{-9}	1.7×10^{-10}	7.2×10^{-28}	[a] 1.3×10^{-4}	10*a*
$[n\text{-}Bu_4N]_4[Mo_8Cu_{12}O_8S_{24}]$	Twenty-nuclear cage	2.3×10^{-9}	-2.5×10^{-8}	8.2×10^{-10}	5.7×10^{-28}	[b] 8.0×10^{-4}	14
$[MoAu_2S_4(AsPh_3)_2]$	Linear	5.1×10^{-10}	-3.6×10^{-9}	-	3.0×10^{-29}	[b] 6.4×10^{-4}	13*b*
$[WAu_2S_4(AsPh_3)_2]$	Linear	7.0×10^{-10}	7.1×10^{-9}	-	6.5×10^{-29}	[b] 5.4×10^{-4}	13*b*
$\{[Et_4N]_2[MoS_4Cu_4(CN)_4]\}_n$	Three-dimensional framework polymer	1.5×10^{-9}	1.3×10^{-8}	4.58×10^{-9}	1.15×10^{-29}	[d] 3.64×10^{-5}	16*a*
$\{[Et_4N]_2[WS_4Cu_4(CN)_4]\}_n$	Three-dimensional framework polymer	1.6×10^{-9}	8.6×10^{-9}	5.12×10^{-9}	1.26×10^{-29}	[d] 2.93×10^{-5}	16*a*
$[Et_4N]_2[MoS_4Cu_4(SCN)_4(2\text{-pic})_4]$	Planar 'open'	3.2×10^{-9}	-6.0×10^{-8}	8.9×10^{-10}	1.29×10^{-31}	[d] 7.44×10^{-4}	15*b*
$[Et_4N]_2[WS_4Cu_4(SCN)_4(2\text{-pic})_4]$	Planar 'open'	3.1×10^{-9}	-4.9×10^{-8}	6.5×10^{-10}	9.42×10^{-32}	[d] 6.98×10^{-4}	15*b*
$[MoS_4Cu_4Br_2(py)_6]$	Planar 'open'	1.5×10^{-9}	1.3×10^{-8}	4.62×10^{-9}	1.17×10^{-30}	[d] 3.8×10^{-4}	This work
$[WS_4Cu_4Br_2(py)_6]$	Planar 'pen'	1.6×10^{-9}	7.8×10^{-9}	5.0×10^{-9}	1.27×10^{-30}	[d] 2.83×10^{-4}	This work
$[MoS_4Cu_4I_2(py)_6]$	Planar 'open'	1.00×10^{-9}	1.8×10^{-8}	5.9×10^{-9}	5.8×10^{-30}	[d] 1.39×10^{-4}	This work
$[WS_4Cu_4I_2(py)_6]$	Planar 'open'	2.55×10^{-9}	8.2×10^{-9}	6.2×10^{-9}	6.9×10^{-30}	[d] 5.5×10^{-4}	This work

[a] In CH_3CN, [b] In CH_2Cl_2, [c] In acetone, [d] In DMF.

clusters contain, the more enhanced is the third-order NLO capability.

Optical limiting (OL) capabilities:

The presence of very strong nonlinear optical absorption effects in clusters **1–4** may significantly enhance the overall OL performance of these four clusters. The optical limiting effects of clusters **1–4** are depicted in Fig. 8. The linear and nonlinear transmission data (filled triangles **1**, open squares **2**, filled diamonds **3**, open circles **4**) were measured at a concentration of 5.50×10^{-4} **1**; 1.39×10^{-4}, **2**; 2.83×10^{-4}, **3**; and 3.8×10^{-4}, **4** mol dm^{-3} DMF solution. Fig. 8 shows that at very low incident fluence, the transmittance is normalized to the linear transmittance for each cluster solution with Beer's law being observed. The light energy transmitted starts to deviate from Beer's law of a linear response when the input light fluence reaches certain values with respect to each cluster, and the solution became increasingly less transparent as the incident fluence rose. Experiments with DMF solvent alone afforded no detectable OL effect. This indicates that solvent contributions are negligible. The values of the limiting threshold, which is defined as the incident fluence at which the actual transmittance falls to 50% of the corresponding linear transmittance, were measured as 0.07 J cm^{-2} **1**, 0.08 J cm^{-2} **2**, 0.08 J cm^{-2} **3**, 0.10 J cm^{-2} **4**, with the same linear transmittances of 72%, respectively.

These large optical limiting effects of the above four heterothiometallic clusters can also be simulated by using excited-state absorption theory.[23] The incident pulsed laser was considered to have a Gaussian distribution both temporally and transversely. The optical limiting curves can be fitted by eqns. (1) and (2), where, $I_s = h\gamma/\sigma_0\tau_{e0}$ were calculated as 0.8×10^9 W cm^{-2} **1**, 1.0×10^9 W cm^{-2} **2**, 1.4×10^9 W cm^{-2} **3**, 1.5×10^9 W cm^{-2} **4**, respectively, based on the eqns. (1) and (2), and τ_{e0} is the lifetime of the excited-state, $K_\alpha = \sigma_e/\sigma_0$ is the ratio of the excited-state absorption cross-section to the ground-state absorption cross-section. The parameters adopted in the numerical calculation were $K_\alpha = 28$ **1**, 25 **2**, 25 **3**, 20 **4**, respectively, which means that the ratio of the triplet excited-state absorption cross-section to the ground-state absorption cross-section of cluster **1** is greater than that of its corresponding isomorphous cluster **2**, while that of cluster **3** is greater than that of cluster **4**, and resulting in the excited-state absorption capability of clusters **1**, **3** being obviously stronger than that of clusters **2**, **4**, respectively. This fact implies that the cluster samples are excited by nanosecond duration laser pulses and that for a given cluster skeleton, the increment in excited-state absorption may arise from heavy atom effects (such as replacing the Mo atom with the heavier W atom, and the Br atom by the heavier I atom). Such a significant improvement of the excited-state absorption gives rise to an increase in the optical limiting performance of these heterothiometallic clusters. In Fig. 8, the solid lines and the dashed lines represent the theoretical lines of the OL effects of clusters **1–4**, by using the eqns. (1) and (2), which fit the OL experimental results well.

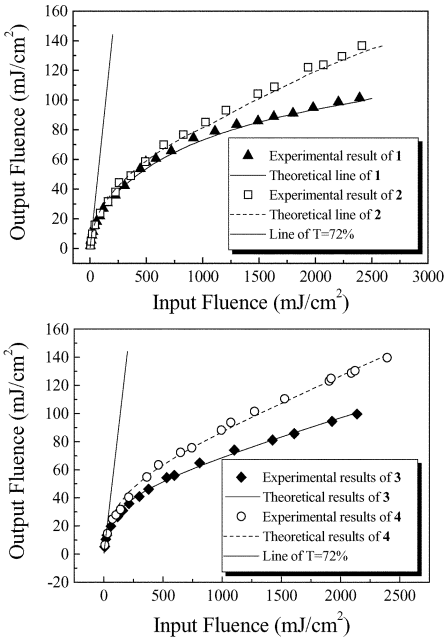

Fig. 8 Optical limiting effects of $[WS_4Cu_4I_2(py)_6]$ **1** (5.50×10^{-4} mol dm^{-3} in DMF) and $[MoS_4Cu_4I_2(py)_6]$ **2** (1.39×10^{-4} mol dm^{-3} in DMF) (upper), and optical limiting effects of $[WS_4Cu_4Br_2(py)_6]$ **3** (2.83×10^{-4} mol dm^{-3} in DMF) and $[MoS_4Cu_4Br_2(py)_6]$ **4** (3.8×10^{-4} mol dm^{-3} in DMF) (lower). The solid and dashed lines are the theoretical fit to the OL experimental results of clusters **1–4** respectively, based on eqns. (1) and (2). The straight lines are a guide to the eye for the situation where Beer's law is obeyed, and with 72% transmittance.

To gain a further insight into the nonlinear origin of these clusters, we have conducted pump–probe experiments. A frequency-doubled Nd : YAG pulse laser with a 532 nm wavelength and 8 ns pulse width was used as a pump beam (pulse energy of 300 μJ). A CW He–Ne laser with wavelength of 632.8 nm was used as a probe beam (optical power of 20 mW). Both the pump and probe beams were collinearly passed through a sample in DMF solution of the clusters with a thickness $L = 0.5$ cm. The probe beam passed through a stopping filter at 532 nm, and was directed into a photometer. When the probe beam (632.8 nm) passed through the photometer, the probe intensity was measured as a function of time with a rapid multiplier phototube connected to a BOXCAR. The change of the probe beam intensity *versus* the delay time was recorded after the pump beam. Experimental curves are shown in Fig. 9. The optical nonlinearities of fullerene-C_{60} were studied by using the same experimental setup. Fullerene-C_{60} exhibits a typically excited-state nonlinearity. Fig. 9 also shows a comparison of pump–probe results for cluster **1** and fullerene-C_{60}. Rapid decreasing of the transmittances of cluster **1** and fullerene-C_{60} indicates that the cluster has a rapid optical response, which is similar to that of fullerene-C_{60}. The time interval between two adjacent points is 80 ns. The lifetime of the triplet state are about 400 ns for fullerene-C_{60} and cluster **1**. Therefore, we can reasonably conclude that the origins of the nonlinearity of the clusters are similar to those for fullerene-C_{60} and the experiment demonstrates that the OL abilities of the clusters mainly arises from excited-state absorption processes.

It is interesting to compare these four clusters **1–4** with other well-known optical limiting materials. Table 4 displays the optical limiting thresholds of clusters **1–4**, cubane-like shaped clusters, nest-shaped clusters, hexagonal prism-shaped cluster, cluster polymers, fullerene-C_{60} and phthalocyanine derivatives.

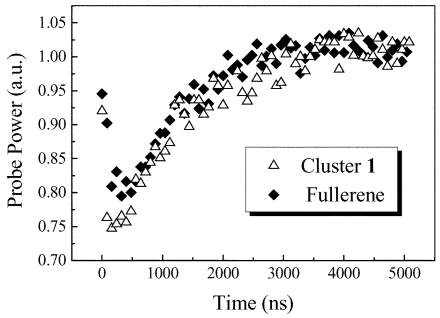

Fig. 9 Pump–probe experimental results for cluster **1** in DMF solution and fullerene C_{60} in toluene solution; the pump fluence is 300 μJ.

Table 4 The limiting thresholds of some OL materials measured at 532 nm with ns laser pulses

Compound	Structure	Solvent	Linear transmission (%)	Limiting threshold/ J cm^{-2}	Ref.
C_{60}	—	Toluene	62	1.6	5*b*
$[Bu_4N]_3[WS_4Cu_3Br_4]$	Cubane-like	MeCN	70	1.1	8*a*,*b*
$[Bu_4N]_3[WS_4Ag_3Br_4]$	Cubane-like	MeCN	70	0.6	8*a*,*b*
$[Bu_4N]_3[MoS_4Ag_3BrI_3]$	Cubane-like	MeCN	70	0.5	7*a*
$[Bu_4N]_3[MoS_4Ag_3Br_4]$	Cubane-like	MeCN	72	0.7	8*b*
$[Bu_4N]_3[MoS_4Ag_3BrCl_3]$	Cubane-like	MeCN	70	0.6	7*a*
$[Bu_4N]_2[MoOS_3Cu_3(NCS)_3]$	Nest shaped	MeCN	71	7	11*c*
$[Bu_4N]_2[MoOS_3Cu_3BrCl_2]$	Nest shaped	MeCN	73	10	11*a*
$[Et_4N]_4[Mo_2O_2S_6Cu_6Br_2I_4]$	Twin-nest shaped	MeCN	70	2	12*b*
$[MoOS_3Cu_3(PPh_3)_3\{S_2P(OBu)_2\}]$	Open cubane-like	CH_2Cl_2	90	5	8*c*
$[MoS_4Ag_3(PPh_3)_3\{S_2P(OBu)_2\}]$	Open cubane-like	CH_2Cl_2	90	0.8	8*c*
$[MoS_4Cu_6I_4(py)_4]_n$	Two-dimensional network polymer	DMSO	—	0.6	16*b*
$\{[Et_4N]_2[MoS_4Cu_4(CN)_4]\}_n$	Three-dimensional framework polymer	DMF	70	0.28	16*a*
$\{[Et_4N]_2[WS_4Cu_4(CN)_4]\}_n$	Three-dimensional framework polymer	DMF	70	0.15	16*a*
Phthalocyanine derivatives	—	Toluene	85	0.1	6*b*
$[Mo_2Ag_4S_8(PPh_3)_4]$	Hexagonal-prism	MeCN	92	0.1	10*b*
$[Et_4N]_2[MoS_4Cu_4(SCN)_4(2\text{-pic})_4]$	Planar 'open'	DMF	84	0.5	15*b*
$[Et_4N]_2[WS_4Cu_4(SCN)_4(2\text{-pic})_4]$	Planar 'open'	DMF	86	0.3	15*b*
$[MoS_4Cu_4Br_2(py)_6]$	Planar 'open'	DMF	72	0.10	This work
$[WS_4Cu_4Br_2(py)_6]$	Planar 'open'	DMF	72	0.08	This work
$[MoS_4Cu_4I_2(py)_6]$	Planar 'open'	DMF	72	0.08	This work
$[WS_4Cu_4I_2(py)_6]$	Planar 'open'	DMF	72	0.07	This work

From the perspective of the optical limiting capability, clusters **1–4** with a planar 'open' skeleton are superior to C_{60} [5*b*] and the cubane-like shaped clusters[7*a*,8] we studied previously, while their OL effects are comparable to phthalocyanine derivatives[6*b*] and the hexagonal prism-shaped cluster $[Mo_2Ag_4S_8(PPh_3)_4]$,[10*b*] and among the best optical limiting materials to date. This may be due to the fact that the planar 'open' skeleton clusters have higher symmetry than the cubane-like shaped clusters and hexagonal prism-shaped cluster, as found in phthalocyanine systems,[5*c*] from decreasing the probability of ground state electronic transitions and giving a smaller absorption cross-section σ_0 and a larger σ_e/σ_0 ratio. It also shows that the optical limiting ability of cluster **1** is stronger than that of cluster **2** and that cluster **3** is stronger than that of cluster **4**. Also, the limiting threshold of cluster **3** is higher than that of cluster **1** and that of cluster **4** is higher than that of cluster **2**. This improvement of the optical limiting ability by replacing skeleton Mo by W or constituent element Br with I implies a heavy atom effect. The importance of the heavy atom effect to the efficiency of nonlinear absorption has already been noticed for metallophthalocyanine systems.[29] This is consistent with the fact that the OL effects of Ag-containing clusters are always better than their Cu-containing homologues. The obvious nonlinearity enhancement may result from the fact that the W- or Ag-containing cluster molecules have much lower pump energy than their corresponding Mo- or Cu-containing counterparts, and hence a plasma of the W- and Ag-containing cluster molecules may be more easily generated, which may result in better optical limiting effects for a given skeleton structure. Such a capability may make the heterothiometallic clusters with pentanuclear planar 'open' MS_4Cu_4 aggregates, as represented by clusters **1–4**, very promising candidates for optical limiting applications.

In summary, we have synthesized and characterized a series of heterothiometallic clusters with planar 'open' skeletons. The strong NLO absorption properties and the optical self-focusing behaviors as well as their superior OL effects for this series of clusters were found when compared with those of the well-known NLO materials. It is demonstrated that in this type of NLO materials, substitution of the skeleton metal atoms or the constituent elements and alternation of the core structure may give rise to the modification of the NLO properties. Time-resolved pump–probe experiments were conducted on these clusters to give direct evidence on the physical origin of the observed OL effects, and these OL effects were also simulated and discussed by using excited-state absorption theory. Thus it is reasonable to conclude that certain optical properties can be obtained through objective molecular design and synthesis.

Acknowledgement

Dr. C. Zhang greatly appreciates the Alexander von Humboldt Foundation for awarding a Humboldt Research Fellowship. This research was supported by the National Science Foundation of China, Foundation from Department of Energy of U.S.A., Foundation of Harbin Institute of Technology, the Malaysian Government and Universiti Sains Malaysia for research grant R & D.

References

1 (*a*) L. W. Tutt and T. F. Boggess, *Prog. Quantum Electron.*, 1993, **17**, 299; (*b*) *Molecular Nonlinear Optics*, ed. J. Zyss, Academic Press, New York, 1994; (*c*) *Nonlinear Optics of Organic Molecules and Polymers*, ed. H. S. Nalwa and S. Miyata, CRC Press, New York, 1997.

2 (*a*) A. Miller, K. R. Welford and B. Daino, *Nonlinear Optical Materials and Devices for Applications in Information Technology*, Kluwer Academic Publishers, Dordrecht, The Netherlands, 1993; (*b*) S. P. Karna and A. T. Yeates, *Nonlinear Optical Materials*, American Chemical Society, Washington, DC, 1996; (*c*) S. R. Marder, B. Kippelen, A. K. Y. Jen and N. Peyghambarian, *Nature*, 1997, **388**, 845; (*d*) R. Syms and J. Cozens, *Optical Guided Waves and Devices*, McGraw-Hill, London, 1993; (*e*) I. R. Whittall, A. M. McDonagh, M. G. Humphrey and M. Samoc, *Adv. Organomet. Chem.*, 1999, **43**, 349.

3 (*a*) *Conference on Laser and Electro-optics*. Technical Digest Series, Optical Society of America, Washington, DC, 1993; (*b*) S. R. Marder, J. E. Sohn and G. D. Strucky, *Materials for Nonlinear Optics, Chemical Perspectives*, American Chemical Society, Washington DC, 1991; (*c*) R. Crane, K. Lewis, E. W. Van Stryland and M. Khoshnevisan, *MRS Symp. Proc. (Mater. Opt. Limit.)*, 1995, 374; (*d*) P. Hood, R. Pachter, K. Lewis, J. W. Perry, D. Hagan and R. Sutherland, *MRS Symp. Proc. (Mater. Opt. Limit. II)*, 1998, 479.

4 (*a*) *Nonlinear Optical Properties of Organic Molecules and Crystals*, ed. D. S. Chemla and J. Zyss, Academic Press, Orlando, FL, 1987; (*b*) *Organic Materials for Nonlinear Optics*, ed. R. A. Hann and D. Bloor, The Royal Society of Chemistry, London, 1991; (*c*) *Optical Nonlinearities and Instabilities in Semiconductors*, ed. H. Huang, Academic Press, Boston, MA, 1988; (*d*) J. L. Bredas, C. Adant, P. Tackx, A. Persoons and B. M. Pierce, *Chem. Rev.*,

1994, **94**, 243.; (*e*) N. J. Long, *Angew. Chem., Int. Ed. Engl.*, 1995, **34**, 21.
5 (*a*) L. W. Tutt and A. Kost, *Nature*, 1992, **356**, 224; (*b*) D. G. McLean, R. L. Sutherland, M. C. Brant, D. M. Brandelik, P. A. Fleitz and T. Pottenger, *Opt. Lett.*, 1993, **18**, 858; (*c*) Y. P. Sun and J. E. Riggs, *Int. Rev. Phys. Chem.*, 1999, **18**, 43.
6 (*a*) J. W. Perry, K. Mansour, I. Y. S. Lee, X. L. Wu, P. V. Bedworth, C. T. Chen, D. Ng, S. R. Mardar, P. Miles, T. Wada, M. Tian and H. Sasabe, *Science*, 1996, **273**, 1533; (*b*) J. W. Perry, K. Mansour, S. R. Marder, K. J. Perry, D. Alvarez Jr. and I. Choong, *Opt. Lett.*, 1994, **19**, 625; (*c*) G. R. Allan, S. J. Rychnovsky, C. H. Venzke and T. F. Boggess, *J. Phys. Chem.*, 1994, **98**, 216; (*d*) I. R. Whittall, A. M. McDonagh, M. G. Humphrey and M. Samoc, *Adv. Organomet. Chem.*, 1998, **42**, 291.
7 (*a*) S. Shi, W. Ji, S. H. Tang, J. P. Lang and X. Q. Xin, *J. Am. Chem. Soc.*, 1994, **116**, 3615; (*b*) P. E. Hoggard, H. W. Hou, X. Q. Xin and S. Shi, *Chem. Mater.*, 1996, **8**, 2218; (*c*) H. W. Hou, H. G. Zheng, H. G. Ang, Y. T. Fan, M. K. M. Low, Y. Zhu, W. L. Wang, X. Q. Xin, W. Ji and W. T. Wong, *J. Chem. Soc., Dalton Trans.*, 1999, 2953.
8 (*a*) S. Shi, W. Ji, J. P. Lang and X. Q. Xin, *J. Phys. Chem.*, 1994, **98**, 3570; (*b*) W. Ji, H. J. Du, S. H. Tang and S. Shi, *J. Opt. Soc. Am. B*, 1995, **12**, 876; (*c*) D. L. Long, S. Shi, X. Q. Xin, B. S. Luo, L. R. Chen, X. Y. Huang and B. S. Kang, *J. Chem. Soc., Dalton Trans.*, 1996, 2617.
9 (*a*) S. Shi, Z. R. Chen, H. W. Hou, X. Q. Xin and K. B. Yu, *Chem. Mater.*, 1995, **7**, 1519; (*b*) Z. R. Chen, H. W. Hou, X. Q. Xin, K. B. Yu and S. Shi, *J. Phys. Chem.*, 1995, **99**, 8717; (*c*) H. W. Hou, B. Liang, X. Q. Xin, K. B. Yu, P. Ge, W. Ji and S. Shi, *J. Chem. Soc., Faraday Trans.*, 1996, **92**, 2343.
10 (*a*) G. Salane, T. Shibahara, H. W. Hou, X. Q. Xin and S. Shi, *Inorg. Chem.*, 1995, **34**, 4785; (*b*) W. Ji, S. Shi, H. J. Du, P. Ge, S. H. Tang and X. Q. Xin, *J. Phys. Chem.*, 1995, **99**, 17297; (*c*) T. Xia, A. Dogariu, K. Mansour, D. J. Hagan, A. A. Said, E. W. Van Stryland and S. Shi, *J. Opt. Soc. Am. B*, 1998, **15**, 1497.
11 (*a*) H. W. Hou, X. R. Ye, X. Q. Xin, J. Liu, M. Q. Chen and S. Shi, *Chem. Mater.*, 1995, **7**, 472; (*b*) P. Ge, S. H. Tang, W. Ji, S. Shi, H. W. Hou, D. L. Long, X. Q. Xin, S. F. Lu and Q. J. Wu, *J. Phys. Chem. B*, 1997, **101**, 27; (*c*) S. Shi, W. Ji, W. Xie, T. C. Chong, H. C. Zeng, J. P. Lang and X. Q. Xin, *Mater. Chem. Phys.*, 1995, **39**, 298.
12 (*a*) H. W. Hou, D. L. Long, X. Q. Xin, X. Y. Huang, B. S. Kang, P. Ge, W. Ji and S. Shi, *Inorg. Chem.*, 1996, **35**, 5363; (*b*) H. W. Hou, X. Q. Xin, J. Liu, M. Q. Chen and S. Shi, *J. Chem. Soc., Dalton Trans.*, 1994, 3211.
13 (*a*) S. Shi, H. W. Hou and X. Q. Xin, *J. Phys. Chem.*, 1995, **99**, 4050; (*b*) H. G. Zheng, W. Ji, M. K. M. Low, G. Sakane, T. Shibahara and X. Q. Xin, *J. Chem. Soc., Dalton Trans.*, 1997, 2357.
14 S. Shi, W. Ji and X. Q. Xin, *J. Phys. Chem.*, 1995, **99**, 894.
15 (*a*) C. Zhang, Y. L. Song, B. M. Fung, Z. L. Xue and X. Q. Xin, *Chem. Commun.*, 2001, 843; (*b*) C. Zhang, Y. L. Song, G. C. Jin, G. Y. Fang, Y. X. Wang, S. S. S. Raj, H. K. Fun and X. Q. Xin, *J. Chem. Soc., Dalton Trans.*, 2000, 1317.
16 (*a*) C. Zhang, Y. L. Song, Y. Xu, H. K. Fun, G. Y. Fang, Y. X. Wang and X. Q. Xin, *J. Chem. Soc., Dalton Trans.*, 2000, 2823; (*b*) H. W. Hou, Y. T. Fan, C. X. Du, Y. Zhu, W. L. Wang, X. Q. Xin, M. K. M. Low, W. Ji and H. G. Ang, *Chem. Commun.*, 1999, 647.
17 J. W. McDonald, G. D. Frieson, L. D. Rosenhein and W. E. Newton, *Inorg. Chim. Acta*, 1983, **72**, 205.
18 G. M. Sheldrick, SADABS, Empirical absorption correction program, University of Gottingen, 1997.
19 M. Sheik-Bahae, D. C. Hutchings, D. J. Hagan and E. W. Van Stryland, *IEEE J. Quantum Electron.*, 1991, **27**, 1296.
20 M. Sheik-Bahae, A. A. Said, T. H. Wei, D. J. Hagan and E. W. Van Stryland, *IEEE. J. Quantum Electron.*, 1990, **26**, 760.
21 (*a*) J. C. Dyason, L. M. Englehardt, P. C. Healy, C. Pakawatchai and A. H. White, *Inorg. Chem.*, 1985, **24**, 1950; (*b*) J. C. Dyason, P. C. Healy, C. Pakawatchai, V. A. Patrick and A. H. White, *Inorg. Chem.*, 1985, **24**, 1957; (*c*) E. W. Ainscough, A. G. Bingham, A. M. Brodie and K. L. Brown, *J. Chem. Soc., Dalton Trans.*, 1984, 989.
22 (*a*) A. Muller, E. Diemann, R. Jostes and H. Bogge, *Angew. Chem., Int. Ed. Engl.*, 1981, **20**, 934; (*b*) E. Diemann and A. Muller, *Coord. Chem. Rev.*, 1973, **10**, 79; (*c*) H. W. Hou, X. Q. Xin and S. Shi, *Coord. Chem. Rev.*, 1996, **153**, 25.
23 (*a*) C. F. Li, L. Zhang, M. Yang, H. Wang and Y. X. Wang, *Phys. Rev. A*, 1994, **49**, 1149; (*b*) G. Y. Fang, Y. L. Song, Y. X. Wang, X. R. Zhang, C. F. Li, L. C. Song and P. C. Liu, *Opt. Commun.*, 2000, **183**, 523.
24 A. A. Said, M. Sherk-Bahae, D. J. Hagan, T. H. Wei, J. Wang, J. Young and E. W. Van Stryland, *J. Opt. Soc. Am. B*, 1992, **9**, 405.
25 M. Sherk-Bahae, A. A. Said and E. W. Van Stryland, *Opt. Lett.*, 1989, **14**, 955.
26 C. Zhang, Y. L. Song, Y. Xu, G. C. Jin, G. Y. Fang, Y. X. Wang, H. K. Fun and X. Q. Xin, *Inorg. Chim. Acta*, 2000, **311**, 25.
27 H. Hashimoto, T. Nakashima, K. Hattori, T. Yamada, T. Mizoguchi, Y. Koyama and T. Kobayashi, *Pure Appl. Chem.*, 1999, **71**, 2225.
28 (*a*) H. Nakanishi, *Nonlinear Optics*, 1991, **1**, 223; (*b*) T. Kobayashi, *IEICE Trans. Fundamental*, 1992, **E75-A**, 38; (*c*) R. Adair, L. L. Chase and S. A. Payne, *Phys. Rev. B*, 1989, **39**, 3337.
29 T. H. Wei, D. J. Hagan, M. J. Sence, E. W. Van Stryland, J. W. Perry and D. R. Coulter, *Appl. Phys. B*, 1992, **54**, 46.